Textual fiducial detection in breast conserving surgery for a near-real time image guidance system

Richey, Winona, Heiselman, Jon, Luo, Ma, Meszoely, Ingrid, Miga, Michael

Winona L. Richey, Jon Heiselman, Ma Luo, Ingrid M. Meszoely, Michael I. Miga, "Textual fiducial detection in breast conserving surgery for a near-real time image guidance system," Proc. SPIE 11315, Medical Imaging 2020: Image-Guided Procedures, Robotic Interventions, and Modeling, 113151L (16 March 2020); doi: 10.1117/12.2550662

SPIE.

Event: SPIE Medical Imaging, 2020, Houston, Texas, United States

Textual fiducial detection in breast conserving surgery for a near-real time image guidance system

Winona L. Richey[1], Jon Heiselman[1], Ma Luo[1], Ingrid M. Meszoely[2], Michael I. Miga[1,3,4,5]

[1] Vanderbilt University, Department of Biomedical Engineering, Nashville, TN USA
[2] Vanderbilt University Medical Center, Division of Surgical Oncology, Nashville, TN USA
[3] Vanderbilt University Department of Radiology and Radiological Sciences, Nashville, TN USA
[4] Vanderbilt Institute for Surgery and Engineering, Nashville, TN USA
[5] Vanderbilt University Medical Center, Department of Neurological Surgery, Nashville, TN USA

ABSTRACT

Breast cancer is the most common cancer in American women, and is the second most deadly. Current guidance approaches for breast cancer surgery provide distance to a seed implanted near the tumor centroid. Large deformations between preoperative imaging and surgical presentation, coupled with the lack of tumor extent information leads to difficulty in ensuring complete tumor resection. Here we propose a novel image guidance platform that utilizes character-based fiducials for easy detection and small fiducial points for precise and accurate localization. Our system is work-flow friendly, and near-real time with use of stereo cameras for surface acquisition. Using simple image processing techniques, the proposed technique can localize fiducials and character labels, providing updates without relying on video history. Character based fiducial labels can be recognized and used to determine correspondence between left and right images in a pair of stereo cameras, and frame to frame in a sequence of images during a procedure. Letters can be recognized with 89% accuracy using the MATLAB built in optical character recognition function, and an average of 81% of points can be accurately labeled and localized. The stereo camera system can determine surface points with accuracy below 2mm when compared to optically tracked stylus points. These surface points are incorporated to a four-panel guidance display that includes preoperative supine MR, tracked ultrasound, and a model view of the breast and tumor with respect to optically tracked instrumentation.

Keywords: breast cancer, lumpectomy, surgical guidance, registration, computer vision, breast conserving surgery, image guided surgery, optical character recognition

1. INTRODUCTION

In the United States, breast cancer is the most commonly diagnosed cancer in women and has the second highest rate of mortality[1]. For women worldwide, breast cancer has the highest incidence and highest morality[2]. Surgery is the standard of care for these patients. Most breast cancer patients are faced with two surgical options: mastectomy or breast conserving therapy (BCT). Mastectomy involves removal of the breast tissue, areola, and skin. While BCT is the removal of the tumor and a margin of healthy tissue surrounding the tumor, with follow-up radiation treatment. Margins are considered negative if there are no tumor cells on the border of the excised mass. Given negative margins, BCT has been shown to have equivalent outcomes to mastectomy[3, 4] with shorter surgical times, shorter post-operative hospital stays, and improved cosmetic outcomes, as the breast usually retains its original shape and symmetry with the contralateral breast[5-9]. High reoperation rates set breast cancer apart from other common general surgeries with an observed versus expected morbidity (O/E) ratio nearly three times higher than that of other general surgeries [10]. In the last six years, BCT reoperation rates have been reported from 8-27%[11-15]. These high rates of positive margins in breast cancer surgeries have been referred to as "the other breast cancer epidemic"[16].

Unfortunately, tumor position and extent can be very difficult to visualize intraoperatively. None of the standard preoperative imaging techniques - mammography, ultrasound, prone magnetic resonance (MR) – have the patient in surgical position. Tumor displacements between imaging position and surgical position are reported between 18 - 68 mm[17-21]. Intraoperative ultrasound (US), which provides tumor extent, has been shown to reduce reoperation rates, but 50% of nonpalpable breast lesions are nonechogenic[22]. Furthermore, it can be difficult to visualize the exact orientation of the US imaging plane, especially for deeper tumors. Current state-of-the-art guidance techniques for breast conserving surgery (BCS) provide distance from a handheld wand to an implanted seed, but do not provide tumor orientation or extent[23-25].

Medical Imaging 2020: Image-Guided Procedures, Robotic Interventions, and Modeling, edited by Baowei Fei, Cristian A. Linte, Proc. of SPIE Vol. 11315, 113151L · © 2020 SPIE
CCC code: 1605-7422/20/$21 · doi: 10.1117/12.2550662

Image guidance solutions are moving towards the use of supine MR and optical tracking[17, 26, 27]. However, these systems do not allow for real time updates. Optically tracked fiducials can only provide surgical planning information, as they must be removed from the breast surface at the start of surgery. We have previously shown retrospectively that tracked fiducials in stereo camera images can provide surface points throughout a video[27]. However, for larger numbers of fiducials, correspondence becomes confounded. High frame rates are used to improve video tracking, and for high numbers of fiducials video processing lags behind real time. While use of a GPU, or more optimized algorithms could reduce processing time, an ideal solution would be independent of video framerate and maintain correspondence even for large numbers of fiducials.

2. METHODS

This work consists of two main components: (1) continual, automated intraoperative monitoring and (2) providing surgeons with tumor location, position and extent before and during BCS. We propose the use of stereo cameras to capture the breast surface in surgery, and we pair these stereo cameras with conventional instrument tracking. This intraoperative monitoring system can be combined with preoperative and intraoperative imaging as well as patient specific models to provide tumor location, position and extent before and during BCS. A four-panel display including MR data, ultrasound data, and a 3D patient specific breast model brings all of the available information into the same space to help the surgeon plan and perform BCS.

Three different skin-tones were painted onto a deformable breast phantom (Breast Probe, SIMULAB Corporation, Seattle, WA). For each skin-tone, the phantom was deformed 4 times using the plungers shown in Figure 1. This resulted in a total of five deformation states: no deformation and deformations from plungers 1-4. Fiducials were marked as small red dots and labels were drawn as blue capital English letters (Figure 1).

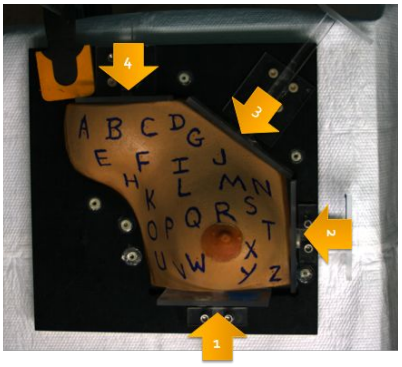

Figure 1: The breast phantom with blue letters and red fiducials; the plungers are indicated with yellow arrows.

Our system uses the Polaris Vicra optical tracker (Northern Digital, Waterloo, ON, Canada) and two Grasshopper cameras (FLIR, formerly Point Grey Research, Richmond, BC, Canada). These two devices are coupled with a rigid bracket as previously presented in [27]. For each deformation state, and for each phantom skin tone, stereo camera images were obtained. Fiducials and their labels were localized with simple thresholding and bounding boxes. These bounding boxes provided image patches. From these image patches, the fiducial location and the letter label were identified. This process is performed in the right and left stereo camera images, and the labels were used to guide correspondence to obtain a set of 3D surface points by triangulation. This process is outlined in Figure 2.

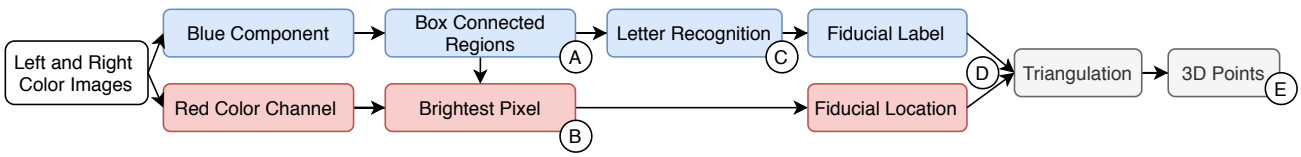

Figure 2: The process to generate three dimensional points from the left and right stereo camera images. Circled letters represent the steps at which results are reported.

To evaluate the accuracy of our system, points obtained from/ the stereo camera images were registered with points manually collected with an optically tracked stylus. These points can then be integrated into a four-panel guidance

display to aid surgeons in visualizing tumor location. Our four-panel image guidance display was implemented using 3D Slicer[28].

2.1 Defining Bounding Boxes

Regions of interest were defined using the blue color component. The blue color component, or the blue percentage of each pixel, was computed with Equation 1.

$$Blue\ Color\ Component = \frac{Blue\ Value}{Red\ Value + Green\ Value + Blue\ Value} \quad (1)$$

Blue pixels have high blue color components, while other colors have lower blue color components. This blue color component allows for easy thresholding of the blue letters, as shown in Figure 3. For example, white pixels are bright in the blue color channel but dark in the blue color component. Case-specific parameters were manually designated including a blue color component threshold, a region of interest outlining the phantom, maximum and minimum bounding box sizes, and padding. The region of interest was used to mask the blue color component image, and the threshold was used to create a binary representation of the blue letter pixels from that masked image. The connected components in this binary image were boxed individually. Boxes that are too big, or too small are removed. This process provides a box around each letter. Parameters were set in the first (non-deformed) frame, and maintained for the remaining 4 images of each experiment.

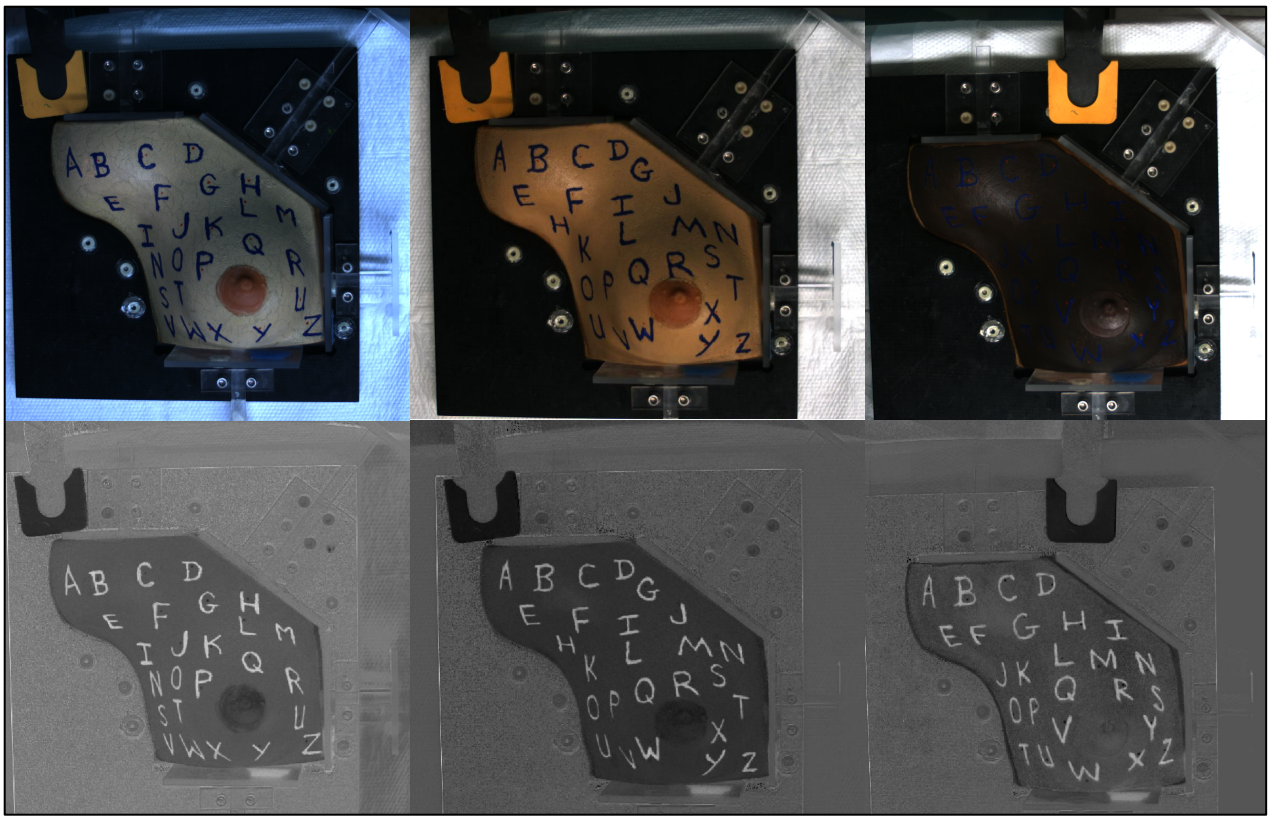

Figure 3: The three phantoms with blue letter labels and red fiducial dots (top row), with their corresponding blue color components (bottom row)

2.2 Fiducial Localization and Labeling

Red pixels display brightly in the red color channel. For each image patch, the brightest pixel in the red color channel is considered the fiducial center and is used as the fiducial's 2D location. This method is fast and reliable. To determine the label for each fiducial, the MATLAB built-in optical character recognition (OCR) method was used. The region inside each bounding box is fed into the OCR function, specifying the limited character set (the alphabet of capital letters), and that the letters are "block" letters. The bounding boxes, with fiducials localized and letters labeled are shown in Figure 4.

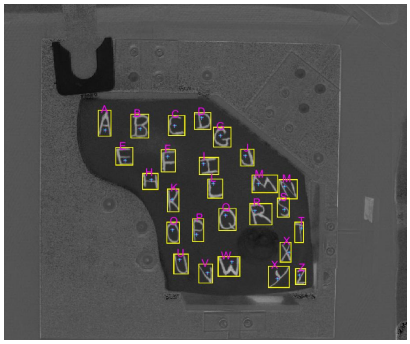

Figure 4: Example output of fiducial and label detection. The blue color component is shown, with boxed connected components in yellow. The fiducial locations are indicated as cyan and magenta asterisks. Letter labels, as output from the letter recognition function, are shown above the image patch in magenta. Here, all labels are correct except for "N", which is mislabeled as "M".

2.3 Generating Labeled 3D points

A very straightforward approach was implemented to handle letter recognition errors. All incorrectly labeled 2D points are not used to triangulate 3D points. When the image patch is labeled as more than one letter or no letter (space), it is considered incorrect. When the incorrect label is a single letter, it can result in a conflict where multiple single-letter labels are identical. With this simplistic correspondence approach, any non-unique single letter label is discarded. For example, if there are two points labeled 'N' in the left image, both those points will not be used, and the point labeled 'N' in the right image will also remain unused; 'N' will not be included in the generated 3D point set. If letter correspondence is incorrect, the triangulated depth is generally quite noticeably an outlier. Therefore, if the triangulated 3D point is more than 3 standard deviations from the mean of the pointset, it is considered an error and discarded. While this approach may seem overly simple, it makes the output points reliable without the need for more complicated error checks.

2.4 Validation

To evaluate the capabilities of our stereo camera system, manual intervention was used to obtain all 26 alphabetical points for all deformation states, on all three phantom skin-tones. Instead of using the automated letter labeling method (OCR), points were manually labeled. For the few cases where there was no bounding box around a letter, the fiducial point was identified manually. This provided a set of 3D points from the stereo camera system. Fiducial locations were also collected manually with an optically tracked stylus (Northern Digital Inc, Waterloo, ON, Canada) and registered to the fiducial locations collected with the stereo camera system**.** This registration defines a transformation matrix, T, consisting of a rotation and transformation to align the two sets of points: $\boldsymbol{x}$, the stereo camera point set, and $\boldsymbol{y}$, the optically tracked point set. $T(\boldsymbol{x})$ represents the stereo camera points that have been transformed into the optically tracked instrumentation space. Fidelity is reported as fiducial registration error (FRE), a measure of overall landmark misalignment, and is shown below, with N representing the number of fiducials, which is 26 for all our trials[29].

$$FRE = \sqrt{\frac{1}{N}\sum_{i=1}^{N}(T(x_i) - y_i)^2} \quad (2)$$

In these experiments, the optically tracked stylus points were considered the gold standard. To evaluate the accuracy of this gold standard, the same fiducial locations on the breast phantom were collected five times with no deformation between collections. Registration was performed with each pair of these validation point sets, and the FRE is reported.

2.5 Four-Panel Display

The points collected with the stereo camera pair inform a four panel display for intraoperative guidance (Figure 5). We propose the use of supine MR performed preoperatively with MR-visible fiducials. This supine MR can be used to generate a patient-specific 3D breast model. The positions of the MR visible fiducials can be marked on the skin with marker (such as the red dot fiducials in Figures 1 and 3), the MR-visible fiducials are removed, and a blue letter label is written beside each dot. During the surgical procedure, the preoperative MR can be registered to the intraoperative surface points collected with our system.

3. RESULTS

This process successfully boxed 99% of letters. Using the reddest pixel to identify the fiducial location was found to be very reliable, as every fiducial that was boxed had a correct fiducial location. This effectiveness can be seen on the histograms in Figure 5A and 5B. Figure 5A shows the histogram of letters that were correctly and completely boxed. Occasionally extraneous boxes were identified, but these boxes were always eliminated at a later step without specific intervention. These extraneous boxes occurred around the edges of our phantoms, mostly near plungers that had entered the region of interest and were reflecting overhead light.

Letters in the blue component image patches were successfully labeled with an average of 89% accuracy, and the accuracy distribution can be seen in Figure 5C. Examples of image patches that were incorrectly labeled are shown in Figure 6. An average of 81% of 3D fiducial points were correctly labeled and localized with the accuracy distribution shown in Figure 6D. To be correctly labeled and localized, the label and red fiducial location must be correct in the left and right images. Incorrect labels lead to confounding correspondence, and were handled as described in section 2.3 to generate 3D points with 73% success rate, as shown in Figure 5E.

The FRE between the stereo camera points and the points manually collected with the optically tracked stylus was 1.9±0.2 mm. The FRE between the five validation point sets manually collected with the optically tracked stylus was 1.4±0.1 mm.

Figure 7 displays a sample of the image guidance system with human data, gathered with IRB approval and patient consent. Using optically tracked tools, instruments can also be registered to and displayed in model space, as shown by the black stylus, and the orange transparent model of the tracked ultrasound plane.

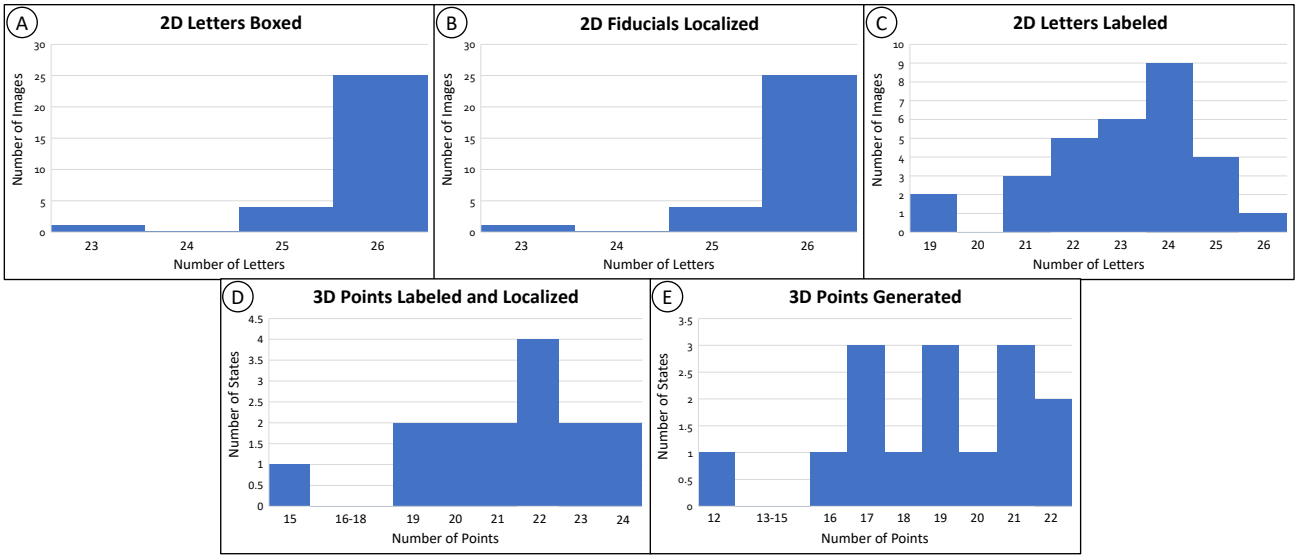

Figure 5: Accuracy at five steps in the process of identifying fiducial points on our phantoms. Circled letters correspond to the locations of circled letters in the steps shown in Figure 2. The top row (A-C) shows metrics all in 2D space, considering left and right frames individually, for a total of 30 frames (3 phantoms, 5 deformation states each, and a left and right image for each state). The y-axes for the top row are number of images. The bottom row (D and E) shows metrics all in 3D space, considering triangulated points, for a total of 15 point sets (3 phantoms, 5 deformation states each).

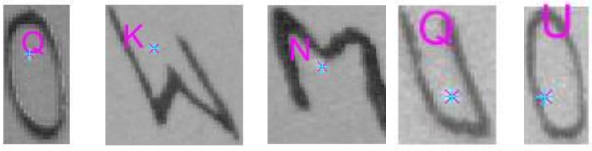

Figure 6: Examples of blue color component image patches that were fed into the optical character recognition function and mislabeled. The output label is displayed in magenta. The fiducial location, as determined by the brightest pixel in the red color channel (not shown), is indicated with a cyan and magenta asterisk.

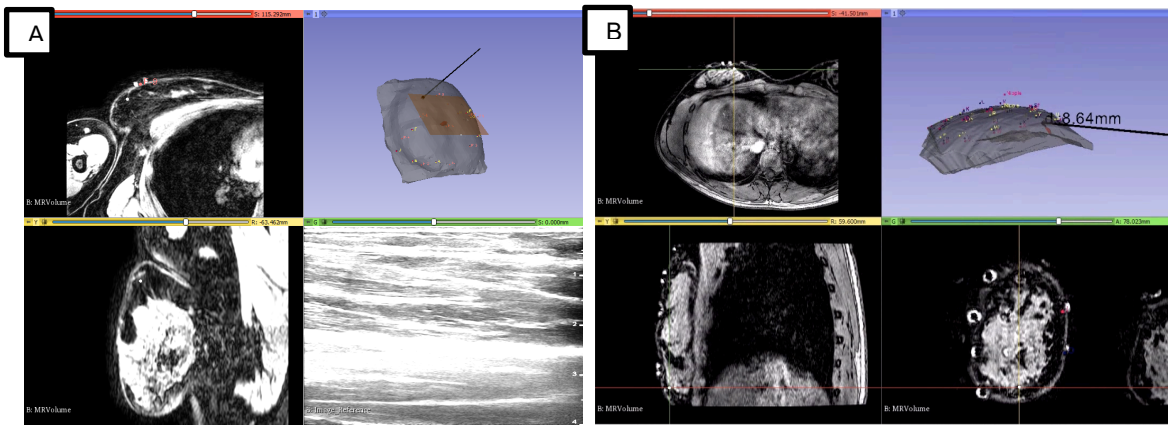

Figure 7: Image guidance system four-panel displays. (A) Display using tracked US probe: MR axial and sagittal slice views (left), live ultrasound feed (right bottom) and 3D rendering, with tumor segmentation in red, surface points, stylus in black, and model of the tracked ultrasound plane in transparent orange (right top). (B) Display using tracked stylus: MR axial, sagittal and coronal slice views each with cross-hair positioning of the tracked stylus (left top, left bottom, right bottom, respectively), and model of the breast, tumor, and tracked stylus with surface points and the distance from stylus to tumor (top right)

4. DISCUSSION

To the best of our knowledge, this work presents the novel use of lettered fiducials in a stereo camera system. Stereo cameras are out of the surgical field, and can measure the surgical position without the use of a seed or probe. Because the field is monitored with RGB cameras, fiducials can be drawn on to the skin with marker. Drawn fiducials are cheap, sterile, and do not interfere with surgical incisions.

Character based fiducial labels allow detection to substitute for tracking, eliminating the need for object history. With each frame processed independently, frames need not be processed in order, or at high frame rates. This allows the system to provide intraoperative surface points at near real time speed, while continuously updating a guidance display with each set of collected points. Letters also provide intuitive features on a previously featureless surface. These letters serve as easy reference points between the patient on the table and the tumor and breast models on the screen.

Letters also allow us to leverage existing work in Optical Character Recognition (OCR) – a large image processing field. The letters in these digital images can be isolated and recognized, applying this existing OCR knowledge to help localize fiducials. Letters are relatively easy to detect, and can be drawn large in size to improve detection while fiducial points can be drawn as small points nearby for accurate and precise fiducial location measurements.

We also present a novel four panel display including tracked ultrasound, registered preoperative MR, and a patient specific 3D breast model in a module written for 3D Slicer[28]. While standard directions treat the breast surface as a clock face to give angle and distance relative to the nipple, letters allow for the addition of more intuitive directions relative to more proximal concrete landmarks. The tracked stylus, displayed with respect to the patient specific breast and tumor models, can be used to help understand lesion, extent, position and depth with respect to the surface by means of the nearby letter landmarks.

While paint was used for our experiments, we propose the use of indelible markers for use on human skin, similar to the markers that are currently used for surgical planning. For the use of this system during surgery, other colors may be more suitable than red, to reduce the impact of blood in the image. We expect this method to be similarly successful using other colored fiducials, particularly with the use of other color channels, and other color spaces. Future work may benefit from green fiducials in the green color channel, or the use of the hue saturation value color space.

While these results show promise, we acknowledge there is much room for improvement. The two main sources of error are poor letter recognition and the compounding nature of errors in the left and right images. The nature of stereo cameras requires the cameras to have slightly different perspectives. In our system, the cameras are at an angle that provides great depth perception, but relatively large distortion in letters on steep surfaces, such as the sides of the breast phantom. This

large distortion contributes to many letter recognition errors. These recognition errors are to be expected, as the OCR method implemented in MATLAB is not optimized for letter recognition in grayscale image patches of handwritten letters. These errors could potentially be reduced using another method. Other methods for OCR have achieved high success ranging up to near human-levels of accuracy, even for handwritten text[30, 31]. Letter distortion also means that recognition errors are likely to only occur on one of the two images. Utilizing the left image to inform the right image labels, and vice versa could dramatically improve performance.

Finally, the FRE reported here was affected by the deformable properties of the phantom. These experiments use a nonrigid breast phantom. The deformable properties of our phantom allow us to evaluate how our system is affected by motion and slight variations in letter configuration and lighting. However, the deformable nature of our phantom causes localization error when using the optically tracked stylus, as the stylus tip needs to be positioned touching the surface without deforming the surface. The registration error between our stylus collected validation point sets was 1.4±0.1 mm. This means that the majority of the error in our stereo camera evaluation, is actually from our validation method, and our cameras are capable of getting reasonably accurate points. Furthermore, conventional optical tracking is widely accepted and used in image guidance. The proposed method of intraoperative surface acquisition performs with comparable accuracy but with significantly reduced workflow interruption.

5. CONCLUSION

This stereo camera system can accurately localize surface points with 1.9±0.2 mm FRE when compared to points manually collected with an optically tracked stylus. On average, 23 of 26 letters correctly (89%) can be detected and labeled correctly. The system can correctly detect and label 21 three-dimensional points (81%). Using this simplistic approach to handling mislabeling, an average of 19 fiducials (73%) can be generated as labeled 3D points with a minimum of 12 fiducials. While 12 fiducials is enough for a rigid registration, more fiducials would provide more information and better alignment between image and physical space. More exploration is necessary to investigate improved approaches and robustness to lighting variations and obstruction. While still in preliminary stages, this system has the potential to be the first continually updating image guidance system for breast cancer surgery.

ACKNOWLEDGEMENTS

This work has been supported by NIH-NIBIB awards T32EB021937, R21EB022380, R01EB027498, and NIH-NCI award R01CA162477.

REFERENCES

[1] R. L. Siegel, K. D. Miller, and A. Jemal, "Cancer statistics, 2019," *CA: a cancer journal for clinicians,* vol. 69, no. 1, pp. 7-34, 2019.

[2] F. Bray, J. Ferlay, I. Soerjomataram, R. L. Siegel, L. A. Torre, and A. Jemal, "Global cancer statistics 2018: GLOBOCAN estimates of incidence and mortality worldwide for 36 cancers in 185 countries," *CA: a cancer journal for clinicians,* vol. 68, no. 6, pp. 394-424, 2018.

[3] B. Fisher, S. Anderson, J. Bryant, R. G. Margolese, M. Deutsch, E. R. Fisher, J.-H. Jeong, and N. Wolmark, "Twenty-year follow-up of a randomized trial comparing total mastectomy, lumpectomy, and lumpectomy plus irradiation for the treatment of invasive breast cancer," *New England Journal of Medicine,* vol. 347, no. 16, pp. 1233-1241, 2002.

[4] J. Vila, S. Gandini, and O. Gentilini, "Overall survival according to type of surgery in young (≤ 40 years) early breast cancer patients: a systematic meta-analysis comparing breast-conserving surgery versus mastectomy," *The Breast,* vol. 24, no. 3, pp. 175-181, 2015.

[5] S. Agarwal, L. Pappas, L. Neumayer, K. Kokeny, and J. Agarwal, "Effect of breast conservation therapy vs mastectomy on disease-specific survival for early-stage breast cancer," *JAMA surgery,* vol. 149, no. 3, pp. 267-274, 2014.

[6] S. P. Bagaria, N. Wasif, B. Rawal, S. A. McLaughlin, and A. E. Giuliano, "Is mastectomy undertreatment for low-risk breast cancers eligible for breast-conserving therapy?," *Cancer,* vol. 121, no. 16, pp. 2705-2712, 2015.

[7] M. B. El-Tamer, B. M. Ward, T. Schifftner, L. Neumayer, S. Khuri, and W. Henderson, "Morbidity and mortality following breast cancer surgery in women: national benchmarks for standards of care," *Annals of surgery,* vol. 245, no. 5, p. 665, 2007.

[8] S. Hofvind, Å. Holen, T. Aas, M. Roman, S. Sebuødegård, and L. Akslen, "Women treated with breast conserving surgery do better than those with mastectomy independent of detection mode, prognostic and predictive tumor characteristics," *European Journal of Surgical Oncology,* vol. 41, no. 10, pp. 1417-1422, 2015.

[9] E. S. Hwang, D. Y. Lichtensztajn, S. L. Gomez, B. Fowble, and C. A. Clarke, "Survival after lumpectomy and mastectomy for early stage invasive breast cancer," *Cancer,* vol. 119, no. 7, pp. 1402-1411, 2013.

[10] D. L. Eck, S. L. Koonce, R. F. Goldberg, S. Bagaria, T. Gibson, S. P. Bowers, and S. A. McLaughlin, "Breast surgery outcomes as quality measures according to the NSQIP database," *Ann Surg Oncol,* vol. 19, no. 10, pp. 3212-7, Oct 2012.

[11] A. A. H. Gladden, S. Sams, A. Gleisner, C. Finlayson, N. Kounalakis, P. Hosokawa, R. Brown, T. Chong, D. Mathes, and C. Murphy, "Re-excision rates after breast conserving surgery following the 2014 SSO-ASTRO guidelines," *The American Journal of Surgery,* vol. 214, no. 6, pp. 1104-1109, 2017.

[12] L. Hughes, J. Hamm, C. McGahan, and C. Baliski, "Surgeon volume, patient age, and tumor-related factors influence the need for re-excision after breast-conserving surgery," *Annals of surgical oncology,* vol. 23, no. 5, pp. 656-664, 2016.

[13] L. Langhans, M.-B. Jensen, M.-L. M. Talman, I. Vejborg, N. Kroman, and T. F. Tvedskov, "Reoperation rates in ductal carcinoma in situ vs invasive breast cancer after wire-guided breast-conserving surgery," *JAMA surgery,* vol. 152, no. 4, pp. 378-384, 2017.

[14] M. T. van Leeuwen, M. O. Falster, C. M. Vajdic, P. J. Crowe, S. Lujic, E. Klaes, L. Jorm, and A. Sedrakyan, "Reoperation after breast-conserving surgery for cancer in Australia: statewide cohort study of linked hospital data," *BMJ open,* vol. 8, no. 4, p. e020858, 2018.

[15] A. M. Zysk, K. Chen, E. Gabrielson, L. Tafra, E. A. M. Gonzalez, J. K. Canner, E. B. Schneider, A. J. Cittadine, P. S. Carney, and S. A. Boppart, "Intraoperative assessment of final margins with a handheld optical imaging probe during breast-conserving surgery may reduce the reoperation rate: Results of a multicenter study," *Annals of surgical oncology,* vol. 22, no. 10, pp. 3356-3362, 2015.

[16] H. S. Cody, 3rd and K. J. Van Zee, "Reexcision--The Other Breast Cancer Epidemic," *N Engl J Med,* vol. 373, no. 6, pp. 568-9, Aug 6 2015.

[17] M. J. Pallone, S. P. Poplack, H. B. Avutu, K. D. Paulsen, and R. J. Barth, Jr., "Supine breast MRI and 3D optical scanning: a novel approach to improve tumor localization for breast conserving surgery," *Ann Surg Oncol,* vol. 21, no. 7, pp. 2203-8, Jul 2014.

[18] L. A. Carbonaro, P. Tannaphai, R. M. Trimboli, N. Verardi, M. P. Fedeli, and F. Sardanelli, "Contrast enhanced breast MRI: spatial displacement from prone to supine patient's position. Preliminary results," *European journal of radiology,* vol. 81, no. 6, pp. e771-e774, 2012.

[19] H. Satake, S. Ishigaki, M. Kitano, and S. Naganawa, "Prediction of prone-to-supine tumor displacement in the breast using patient position change: investigation with prone MRI and supine CT," *Breast Cancer,* vol. 23, no. 1, pp. 149-158, 2016.

[20] M. A. Mallory, Y. Sagara, F. Aydogan, S. DeSantis, J. Jayender, D. Caragacianu, E. Gombos, K. G. Vosburgh, F. A. Jolesz, and M. Golshan, "Feasibility of Intraoperative Breast MRI and the Role of Prone Versus Supine Positioning in Surgical Planning for Breast-Conserving Surgery," *Breast J,* vol. 23, no. 6, pp. 713-717, Nov 2017.

[21] E. C. Gombos, J. Jayender, D. M. Richman, D. L. Caragacianu, M. A. Mallory, F. A. Jolesz, and M. Golshan, "Intraoperative supine breast MR imaging to quantify tumor deformation and detection of residual breast cancer: preliminary results," *Radiology,* vol. 281, no. 3, pp. 720-729, 2016.

[22] N. A. Lee, H. Rusinek, J. Weinreb, R. Chandra, H. Toth, C. Singer, and G. Newstead, "Fatty and fibroglandular tissue volumes in the breasts of women 20-83 years old: comparison of X-ray mammography and computer-assisted MR imaging," *AJR. American journal of roentgenology,* vol. 168, no. 2, pp. 501-506, 1997.

[23] V. Mango, R. Ha, A. Gomberawalla, R. Wynn, and S. Feldman, "Evaluation of the SAVI SCOUT surgical guidance system for localization and excision of nonpalpable breast lesions: a feasibility study," *American Journal of Roentgenology,* vol. 207, no. 4, pp. W69-W72, 2016.

[24] S. E. Nolano, L. O. Thalhiemer, E. Yu, E. Grujic, W. B. Carter, and T. G. Frazier, "A comparison of the micro-impulse radar SAVI SCOUT to the radioactive I125 seed in localization of non-palpable breast cancer for breast conserving therapy," (in English), *Cancer Research,* Meeting Abstract vol. 77, p. 2, Feb 2017.

[25] J. R. Harvey, Y. Lim, J. Murphy, M. Howe, J. Morris, A. Goyal, and A. J. Maxwell, "Safety and feasibility of breast lesion localization using magnetic seeds (Magseed): a multi-centre, open-label cohort study," *Breast cancer research and treatment,* vol. 169, no. 3, pp. 531-536, 2018.

[26] R. J. Barth, V. Krishnaswamy, K. D. Paulsen, T. B. Rooney, W. A. Wells, C. V. Angeles, R. A. Zuurbier, K. Rosenkranz, S. Poplack, and T. D. Tosteson, "A Randomized Prospective Trial of Supine MRI-Guided Versus Wire-Localized Lumpectomy for Breast Cancer," *Annals of surgical oncology,* pp. 1-10, 2019.

[27] W. L. Richey, M. Luo, S. E. Goodale, L. W. Clements, I. M. Meszoely, and M. I. Miga, "A system for automatic monitoring of surgical instruments and dynamic, non-rigid surface deformations in breast cancer surgery," in *Medical Imaging 2018: Image-Guided Procedures, Robotic Interventions, and Modeling*, 2018, vol. 10576, p. 105761H: International Society for Optics and Photonics.

[28] A. Fedorov, R. Beichel, J. Kalpathy-Cramer, J. Finet, J.-C. Fillion-Robin, S. Pujol, C. Bauer, D. Jennings, F. Fennessy, and M. Sonka, "3D Slicer as an image computing platform for the Quantitative Imaging Network," *Magnetic resonance imaging,* vol. 30, no. 9, pp. 1323-1341, 2012.

[29] J. M. Fitzpatrick, D. L. Hill, and C. R. Maurer Jr, "Image registration," *Handbook of medical imaging,* vol. 2, pp. 447-513, 2000.

[30] A. Chaudhuri, K. Mandaviya, P. Badelia, and S. K. Ghosh, "Optical Character Recognition Systems for Latin Language," in *Optical Character Recognition Systems for Different Languages with Soft Computing*Cham: Springer International Publishing, 2017, pp. 165-191.

[31] L. Chen, S. Wang, W. Fan, J. Sun, and S. Naoi, "Beyond human recognition: A CNN-based framework for handwritten character recognition," in *2015 3rd IAPR Asian Conference on Pattern Recognition (ACPR)*, 2015, pp. 695-699: IEEE.